Development of Microwave Antenna for ECR Microwave Plasma Production

Camille Faith ROMERO* and Motoi WADA*

(Received January 19, 2016)

Spirally wound antennas for an ECR microwave plasma device have been designed and tested. The antennas were modified in terms of their structures, materials and positions with respect to the magnetic flux density. Antenna performance was assessed based on reflected power, optical emission and Langmuir probe measurements. Results indicated that among the three types of antenna structures: cylindrical, conical and planar circular coil, the last produced the highest H_α emission intensities at ECR condition. It is also observed that launching the microwave at the distance from the flange to the antenna surface, D = 50 mm where $\omega < \omega_{ce}$, produced more intense discharge. Antennas made of nickel and carbon were compared. Though Ni antenna produced denser plasma, the carbon antenna served as an effective carbon radical source generating more carbon and hydrocarbon species.

Key words: microwave plasma, electron cyclotron resonance (ECR), carbon thin film, chemical sputtering

1. Introduction

The demand for low-temperature, low-pressure, high-density plasma discharges in materials processing had driven further development of electron cyclotron resonance (ECR) microwave plasma sources. Sources of this type are widely used in various applications such as semiconductor etching, thin film deposition, ion beam production, and surface treatment [1-3]. These sources realize high degree of ionization, high concentration of reactive particles, and low plasma potential which are advantageous for various applications [2,4].

Properties of microwave generated plasma highly depend on the conditions and methods under which the discharge is created like ECR condition. One important factor that should be considered is the coupling of microwave power to a magnetic field. Microwave couplers or applicators are being utilized for realizing several functions such as: (i) impedance matching and optimization of microwave energy transfer, (ii) enhancement of plasma particle production, and (iii) controllability and uniformity of the plasma density. Microwave applicators that are typically used in ECR reactors include purposely designed antennas, surfatrons, waveguides, and cavity applicators [4,5]. Antennas are radiation transmitters that excites electromagnetic fields in a closed volume like free space wave, without being significantly bounded to certain geometry.

The common feature of power transfer by means of antennas is the injection of microwave into the discharge across a dielectric window to inductively couple electromagnetic power between the coil and the plasma [6-8]. In thin film deposition, antennas such as coils are usually placed behind barriers of dielectric media (e. g. quartz glass) to eliminate the possibility of metal contamination from the antenna due to surface sputtering. For the case of carbon thin film formation, such problem can be prevented if the antenna surface is made of the same material. In this study, series of modifications was done for the structure of nickel antennas to optimize microwave power absorption and achieve high density of radicals and active species. Based on the optimal structure, a carbon antenna was fabricated and used to launch microwaves into the discharge. It was immersed in hydrogen plasma with the presence of dc magnetic field.

* Department of Electronics & Electrical Engineering, Graduate School of Science & Engineering, Doshisha University, Kyoto
E-mail: camillefaith.romero@gmail.com

The performance of the microwave antenna was assessed by qualitative and quantitative diagnostics such as visual inspection and reflected power measurements, respectively. In addition, local in-situ diagnostics such as Langmuir probe analysis and non-invasive diagnostic like optical emission spectroscopy were employed to evaluate the properties and parameters of produced plasma species.

2. Methodology

A schematic diagram of the experimental system used in the study is shown in Fig. 1(a). The reaction chamber of 270 mm in diameter and 340 mm in depth was evacuated by a rotary pump coupled to a 560 l/s turbomolecular pump (TMP) to a base pressure less than 6 × 10^{-7} Torr. H_2 gas was introduced into the chamber through a ring-shaped injection unit located 100 mm from the base of the top flange through a needle valve. A gate valve connecting the chamber to the inlet of the TMP was half-closed to restrict the gas outflow and keep the pressure in the chamber at 8 × 10^{-3} Torr. The gas ring has a solid carbon cylinder inserted in its inner diameter and a carbon disk placed on its nozzles. The ring generates hydrocarbon molecules through chemical sputtering process. Plasma expands into the chamber under the influence of a magnetic field gradient or $\nabla_{+}B \times \boldsymbol{B}$ drift. The magnetic field distribution along the central axis (R = 0 mm) varied according to the current applied to the electromagnet I_B, as seen in Fig. 1(b). The magnetic flux density 87.5 mT was sufficient to produce ECR condition for 2.45 GHz frequency at I_B ≥ 80 A. Continuous 2.45 GHz microwave power was supplied by an integrated generator via a coaxial cable. A three-stub tuner connected to the antenna end of the line wasused to minimize the reflected power. The microwave was launched into the chamber through an antenna which was modified in terms of its structure and material. Nickel wires were cut to configure three types of antenna structure: plane circular, conical and cylindrical coil, as illustrated in Fig. 2.

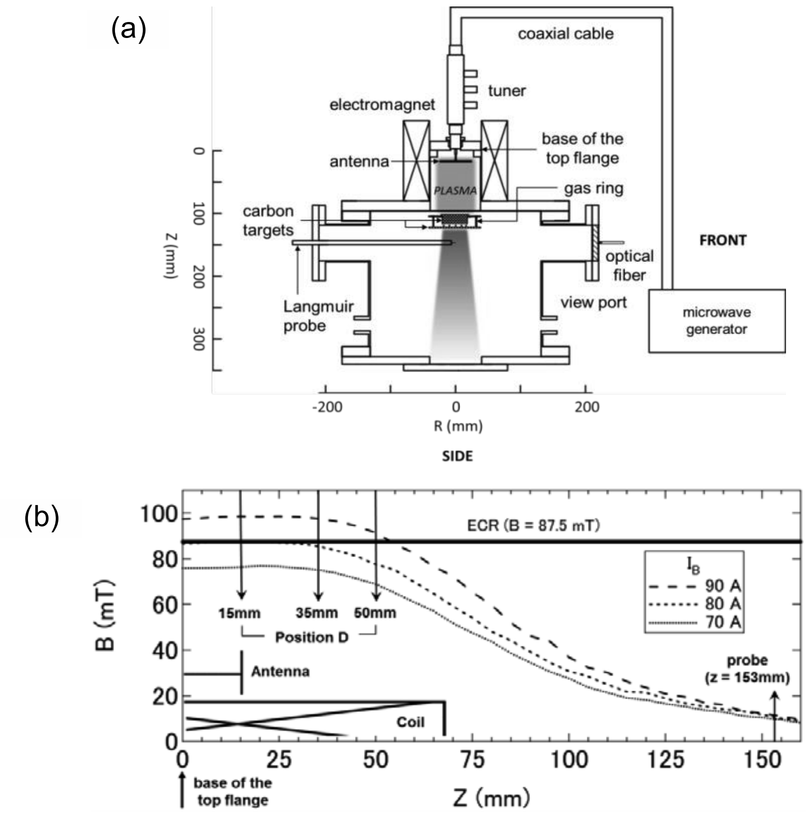

Fig. 1. (a) Schematic diagram of the ECR-PECVD. (b) Axial profile of the magnetic field at R = 0 mm.

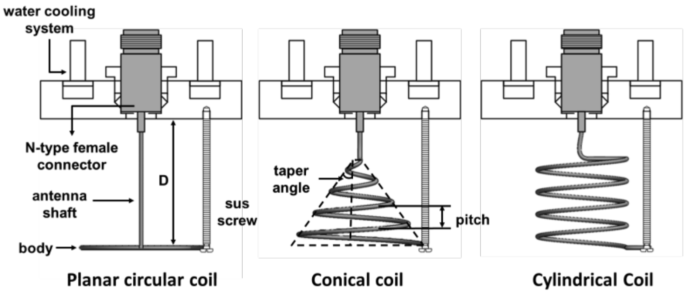

Antenna parameters	Planar		Conical	Cylindrical
Number of turns	2.5	4	4	4
Inner diameter (mm)	13	9	9	37
Outer diameter (mm)	49		49	37
Pitch (mm)	10.5	6.3	10	10
Taper angle (°)	--		37	0
Position D (mm)	50	15 35 50	50	50

Fig. 2. Antenna structure diagrams (front view) with the corresponding parameters.

Each antenna is composed of 4 turns. The wire was wound in a counter-clockwise direction when viewed from the vacuum side. The position of the planar coil antenna, *D*, was varied relative to its distance from the base of the top flange, as indicated in Fig. 1(b). Position *D* was adjusted by changing the length of the antenna shaft. The other end of the antenna was grounded. A 2.5-turn planar coil antenna made of carbon was also fabricated and compared to the nickel planar antenna of the same number of turns. Illustration and measurement of the carbon antenna are shown in Fig. 3.

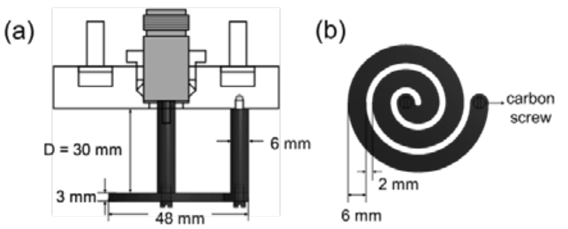

Fig. 3. (a) Front view design of the carbon antennas.
(b) Bottom view.

To test the antenna matching, the reflected power P_R was evaluated from voltmeter readings connected to a built-in coupler. The plasma was characterized by visual inspection, probe measurements and optical emission spectroscopy. Visual observations were supported by photographs taken through a view port with a 14.6 megapixels digital single-lens reflex camera equipped with a 18-55 mm f/3.5-5.6 zoom lens. Pictures were taken with an aperture of f/32, 0.6 seconds exposure time and 800 ISO speed. Ion saturation current I_{sat} was measured with a cylindrical Langmuir probe made of tungsten wire with 5 mm length and 0.5 mm diameter. The probe was inserted 153 mm from the top flange base to travel along an axis to measure plasma parameter distributions radially. Light emission from the plasma was detected through the view port by an optical fiber attached to an Ocean Optics USB4000 spectrometer with 0.2 nm spectral resolution. The fiber sensor head was mounted perpendicularly to the port at the same level with the Langmuir probe where it observes the plasma region right beneath the gas injection unit.

3. Results and Discussions

The dependence of P_R on I_B for different forms of coil antenna is shown in Fig. 4(a). In Fig. 4(b), H_α intensities that provide a hint on the ionized hydrogen content of the plasma are plotted. The input power was set to 100 W. Relatively low reflected power, about 0.1% to 10%, were measured from the three structures in the range I_B = 55 A to 75 A. In this region, while P_R values of the antennas appear to be nearly the same from 45 A to 75 A, characteristic differences were seen in their H_α emission intensities, as displayed in Fig. 4(b). At I_B < 45 A, plasmas are not sustained well due to plasma confinement of a weak magnetic field. The H_α line intensity of planar and cylindrical coil antennas suddenly drops. For the case of the conical coil antenna, it produced much lower H_α emission intensities compared to the other two antenna structures despite of their P_R characteristic resemblances. This event indicates that reflected power measurements do not necessarily determine the power absorbed by the plasma. The absorbed power can be dissipated within the antenna

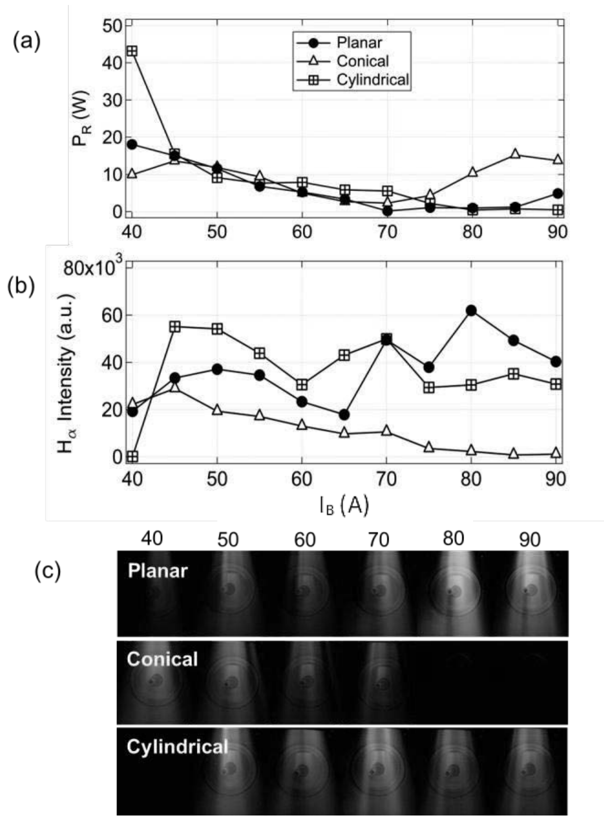

Fig. 4. (a) P_R magnitude, (b) H_α line intensity at 656.3 nm and (c) photos of plasma at varying I_B. for three types of antenna structures.

load itself which can be the case for the conical antenna. Photos of plasmas at changing electro-magnet current are shown in Fig. 4(c). After generation of plasma near the antenna region, the plasma expands into the processing chamber under the influence of magnetic field gradient. This explains the tapered cylinder shape of the plasma produced by the three antennas. Dark bands appear when plasma glow starts to diminish as the separation of radiating spiral arms becomes more apparent.

In the following series of experiments, planar coil antenna was utilized due to its lower P_R and higher H_α emission intensities at ECR condition than that of the other two coil structures. In Fig. 5, H_α emission intensities and ion saturation current, measured by a Langmuir probe, are plotted as functions of I_B for different antenna positions. It can be observed that the injection of microwave at D = 15 mm resulted to low H_α emission intensities and I_{sat} values. This can be accounted to the too large distance from the observation point to the antenna and also to the near top flange walls where plasma particles could have lost. On the other hand, launching microwave at D = 35 mm and 50 mm produced much higher H_α line intensities and I_{sat} values. At 35-mm position, microwave was injected farther than at 50 mm. However, both of their H_α intensity and I_{sat} values are comparable. Hence, the effect of distance from the probe and optical fiber observation point on measurements can be negligible.

When the microwaves were launched in the discharge areas where the magnetic field B < 875 G, that is utilizing: 15 mm, 35 mm and 50 mm at I_B < 80 A, I_B < 80 A, and I_B < 90 A, respectively, the intensity of H_α and I_{sat} value increased. In these regions, where $\omega < \omega_{ce}$, more microwave power absorption of electromagnetic waves can occur resulting to high plasma density [9]. At I_B = 75 A, a recurring sudden change in the H_α and I_{sat} amplitudes was detected. This jump in the plasma parameter was an indication of sub-ECR to ECR mode transition [10].

The effect of antenna material on the performance was also investigated. This time, the 2.5-turn nickel and carbon planar coil antennas were being utilized. Figure 6 shows the dependence of electron temperature, T_e, density, n_e, and P_R on the magnetic field intensity for

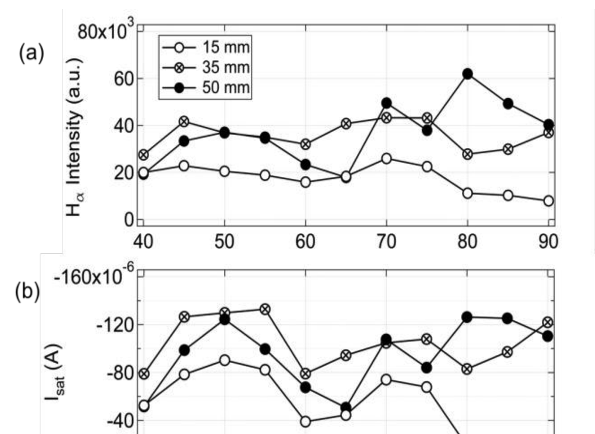

Fig. 5. (a) H_α line intensity at 656.3 nm and (b) I_{sat} measurements at varying I_B.

different antenna materials. In spite of the low P_R values for both Ni and carbon antennas in the range 60 A to 80 A, Ni antenna produced plasma with much higher electron density. A high contact resistance between the carbon antenna and the stainless steel N-type connector may have caused local power dissipation resulting in less power absorption by plasmas. More stable plasma was also observed in Ni-antenna-generated plasma as detected on the P_R and T_e values. At 80 A, the discharge produced by the C antenna had a sudden drop and rise in its P_R and n_e values, respectively. This is an indication of strong microwave absorption in the ECR region near the antenna position at D = 30 mm.

At points where the electron density of the plasma produced by the C antenna was low, the electron temperature rises. This behavior can be a manifestation of unstable plasma wherein the electron temperature tends to be high in order to maintain the plasma [11].

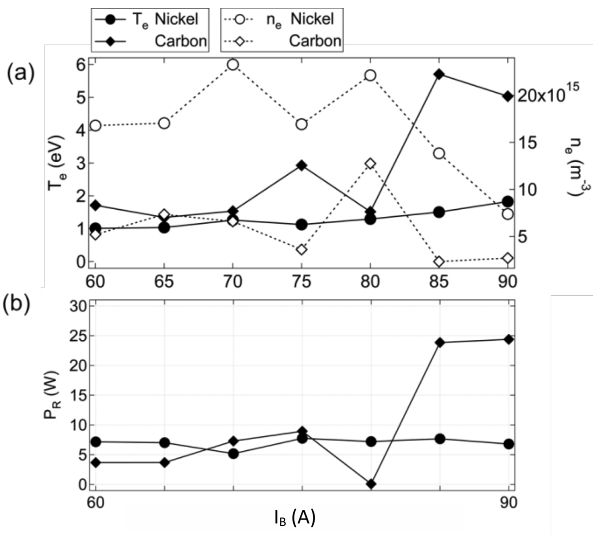

Fig. 6. (a) T_e, n_e values and (b) P_R magnitude at varying I_B for different antenna materials.

The influence of flux density and antenna material on the intensity ratio of CH (387 nm) and C_2 (516 nm) emission lines to H_α (656.3 nm) line is displayed in Fig. 7. At I_B = 80, where high microwave power absorption occured, carbon antenna produced plasma of which CH/H_α and C_2/H_α intensity ratios were almost four times higher than that produced by a Ni antenna. This increase in the carbon and carbon hydride emission was due to chemical sputtering of the carbon antenna by hydrogen plasma.

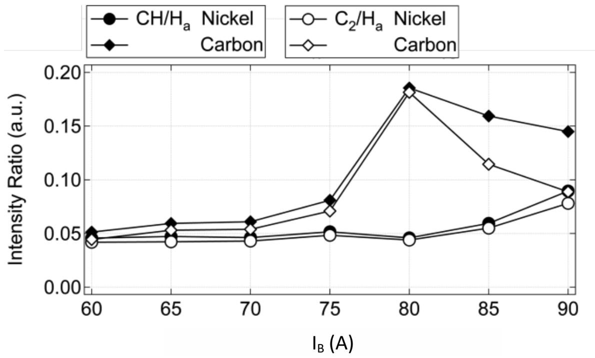

Fig. 7. Intensity ratio of CH and C_2 lines to H_α line at varying I_B for different antenna materials.

4. Summary

Three antenna coil structures were assessed by H_α intensity and probe measurements. High microwave power delivery and absorption was detected in plasmas produced using a planar circular coil. By changing the position of the antenna with respect to the flux density, it was observed that high plasma density can be achieved by launching the microwave in regions where $\omega < \omega_{ce}$. Also, the increase in the carbon and hydrocarbon radical emission in the plasma produced by the carbon antenna has been confirmed by an optical emission spectroscopic analysis.

The obtained results have proven the possibility of utilizing a carbon antenna to serve not only a microwave radiator but also a carbon radical source. Presently, a new carbon antenna is being developed to increase microwave coupling efficiency, prolong plasma operation time and enhance the production of hydrocarbon radicals.

This work has been conducted as the Bilateral Cooperation Research Project supported by the Japan Society for the Promotion of Science, and the Philippines Department of Science and Technology.

References

1) M. A. Lieberman and A. J. Lichtenberg, Principles of Plasma Discharges and Materials Processing (2^{nd} ed.), (John Wiley & Sons, Inc., New Jersey, 2005).
2) C. M. Ferreira and M. Moisan, Microwave Discharges: Fundamentals and Applications, (Plenum Press, New York, 1993).
3) J. Musil, "Deposition of Thin Films Using Microwave Plasmas: Present Status and Trends," *Vacuum*, **47**[2], 145 (1996).
4) O. A. Popov, High Density Plasma Sources: Design, Physics and Performance, (Noyes Publications, New Jersey, 1995).
5) J. Asmussen, "Electron Cyclotron Resonance Microwave Discharges for Etching and Thin-film Deposition," *J. Vac. Sci. Technol. A*, **7**[3], 887 (1989).
6) M. Geisler, J. Kieser, E. Rauchle and P. Wilhelm, "Elongated Microwave Electron Cyclotron Resonance Heating Plasma Source," *J. Vac. Sci. Technol. A,* **8**[2], 908 (1990).
7) N. Sato, S. Iizuka, Y. Nakagawa and T. Tsukada, "Uniform Plasma Produced by a Plane Slotted Antenna with Magnets for Electron Cyclotron Resonance," *Appl. Phys. Lett.*, **62**[13], 1469 (1993).
8) J. Cotrino, A. Palmero and V. Rico, "Electron Temperature Measurement in a Slot Antenna 2.45 GHz Microwave Plasma Source," *J. Vac. Sci. Technol. B*, **19**[2], 411 (2001).
9) M. A. Lieberman and R. A. Gottscho, Physics of Thin Films (Vol. 18), M. H. Francombe and J. L. Vossen, eds. (Academic Press, California, 1994).
10) P. K. Shufflebotham and D. J. Thomson, "Diagnostic Techniques for Plasma Stability in Electron Cyclotron Resonance Plasma Processing," *J. Vac. Sci. Technol. A*, **8**[5], 3716 (1990).
11) N. Itagaki, Y. Ueda, N. Ishii and Y. Kawai, "Production of Low Electron Temperature ECR plasma for Thin Film Deposition," *Surf. Coat. Technol.*, **142-144**, 550 (2001).